Journal of Solid State Chemistry **160,** 409–414 (2001)
doi:10.1006/jssc.2001.9256, available online at http://www.idealibrary.com on IDEAL®

Syntheses and Structures of the Quaternary Copper Tellurides $K_3Ln_4Cu_5Te_{10}$ (*Ln* = Sm, Gd, Er), $Rb_3Ln_4Cu_5Te_{10}$ (*Ln* = Nd, Gd), and $Cs_3Gd_4Cu_5Te_{10}$

Fu Qiang Huang and James A. Ibers[1]

Department of Chemistry, Northwestern University, 2145 Sheridan Rd., Evanston, Illinois 60208-3113

Received February 15, 2001; in revised form May 16, 2001; accepted May 25, 2001; published online July 16, 2001

Six quaternary alkali-metal rare-earth copper tellurides $K_3Ln_4Cu_5Te_{10}$ (*Ln* = Sm, Gd, Er), $Rb_3Ln_4Cu_5Te_{10}$ (*Ln* = Nd, Gd), and $Cs_3Gd_4Cu_5Te_{10}$ have been synthesized at 1123 K with the use of reactive fluxes of alkali-metal halides *A*Cl (*A* = K, Rb, Cs). All crystallographic data were collected at 153 K. These compounds crystallize in space group *Pnnm* of the orthorhombic system with two formula units in cells of dimensions (*A*$_3$*Ln*$_4$, *a*, *b*, *c* (Å)): K_3Sm_4, 16.590(2), 17.877(2), 4.3516(5); K_3Gd_4, 16.552(4), 17.767(4), 4.3294(9); K_3Er_4, 16.460(4), 17.550(4), 4.2926(9); Rb_3Nd_4, 17.356(1), 17.820(1), 4.3811(3); Rb_3Gd_4, 17.201(2), 17.586(2), 4.3429(6); Cs_3Gd_4, 17.512(1), 17.764(1), 4.3697(3). The corresponding R_1 indices for the refined structures are 0.0346, 0.0315, 0.0212, 0.0268, 0.0289, and 0.0411. The three $K_3Ln_4Cu_5Te_{10}$ structures belong to one structure type and the $Rb_3Ln_4Cu_5Te_{10}$ (*Ln* = Nd, Gd) and $Cs_3Gd_4Cu_5Te_{10}$ structures belong to another one, the difference being the location of one of the three unique Cu atoms. Both structure types are three-dimensional tunnel structures that contain similar *Ln*/Te fragments built from $LnTe_6$ octahedra and $CuTe_4$ tetrahedra. The $CuTe_4$ tetrahedra form $^1_\infty[CuTe_3^{5-}]$ and $^1_\infty[CuTe_2^{3-}]$ chains. The alkali-metal atoms, which are in the tunnels, are coordinated to seven or eight Te atoms. © 2001 Academic Press

INTRODUCTION

Compounds that contain a *d*-block metal and an *f*-block metal are of interest because intriguing structural and physical properties may result from the interplay of the covalent transition-metal bonding with the more ionic lanthanide or actinide bonding. Moreover, metal chalcogenide semiconductors, take Cd*Q* (*Q* = S, Se, Te) as an example, have electronic configurations suitable for the formation of Zintl phases with elements from Group 3 (including the rare earths), 4, 5, 11, and 12. The introduction of an alkali metal or alkaline-earth metal may modify the physical properties, dimensional reduction being one example (1, 2). Physical properties in closely related compounds may differ, depending on the alkali metal or alkaline-earth metal (3, 4). A number of compounds that combine these two features, namely contain an *f*-block metal (*Ln*), a *d*-block metal (*M*), a chalcogen (*Q* = S, Se, or Te), and an alkali metal or alkaline-earth metal (*A*), have been synthesized recently (5–21) by the reactive flux method (22, 23). Here we report the syntheses and structural characterization of six new compounds of this kind, namely the quaternary copper tellurides $K_3Ln_4Cu_5Te_{10}$ (*Ln* = Sm, Gd, Er), $Rb_3Ln_4Cu_5Te_{10}$ (*Ln* = Nd, Gd), and $Cs_3Gd_4Cu_5Te_{10}$.

EXPERIMENTAL

Syntheses

The following reagents were used as obtained: Nd (Alfa, 99.9%), Sm (Alfa, 99.9%), Gd (Alfa, 99.9%), Er (Alfa, 99.9%), Cu (Aldrich, 99.999%), Te (Aldrich 99.8%), LiCl (Aldrich, 99.99%), KCl (Aldrich, 99.98%), RbCl (Aldrich, 99.8%), and CsCl (Aldrich, 99.99%). Reaction mixtures of 1.0 mmol *Ln*, 1.0 mmol Cu, and 2.0 mmol Te with 600 mg *A*Cl/LiCl (mole ratio *A*Cl:LiCl = 55:45) were loaded into fused-silica tubes under an Ar atmosphere in a glove box. These tubes were sealed under a 10^{-4} Torr atmosphere and then placed in a computer-controlled furnace. The samples were heated to 1123 K in 16 h, kept at 1123 K for 3 days, cooled at 0.05 K/min to 573 K, and then cooled to room temperature. The reaction mixtures were washed free of chloride salts with water and dried with acetone. The major products in all instances were black needles of the stated compositions of *A*:*Ln*:Cu:Te = 3:4:5:10, as determined to an accuracy of about 5% by the examination of selected single crystals with an EDX-equipped Hitachi S-4500 SEM. Yields were about 70%. The compounds were stable in air for a few weeks.

[1]To whom correspondence should be addressed. E-mail: ibers@chem.northwestern.edu.

0022-4596/01 $35.00

TABLE 1
Crystal Data and Structure Refinements[a] for $K_3Ln_4Cu_5Te_{10}$ (*Ln* = Sm, Gd, Er), $Rb_3Ln_4Cu_5Te_{10}$ (*Ln* = Nd, Gd), and $Cs_3Gd_4Cu_5Te_{10}$

Compound	$K_3Sm_4Cu_5Te_{10}$	$K_3Gd_4Cu_5Te_{10}$	$K_3Er_4Cu_5Te_{10}$	$Rb_3Nd_4Cu_5Te_{10}$	$Rb_3Gd_4Cu_5Te_{10}$	$Cs_3Gd_4Cu_5Te_{10}$
Formula weight	2312.40	2340.00	2380.04	2427.07	2479.11	2621.43
a (Å)	16.590(2)	16.552(4)	16.460(4)	17.356(1)	17.201(2)	17.512(1)
b (Å)	17.877(2)	17.767(4)	17.550(4)	17.820(1)	17.586(2)	17.764(1)
c (Å)	4.3516(5)	4.3294(9)	4.2926(9)	4.3811(3)	4.3429(6)	4.3697(3)
V (Å^3)	1290.6(2)	1273.2(5)	1240.0(5)	1355.0(2)	1313.7(3)	1359.3(2)
ρ_c (g/cm^3)	5.951	6.104	6.375	5.949	6.267	6.405
μ (cm^{-1})	245.24	260.53	295.89	272.48	302.97	279.02
Transmission factors	0.064–0.429	0.132–0.720	0.098–0.428	0.065–0.462	0.116–0.779	0.163–0.682
R_1[b]	0.0346	0.0315	0.0212	0.0268	0.0289	0.0411
wR_2[c]	0.0788	0.0630	0.0478	0.0645	0.0655	0.0955

[a] $T = 153(2)$ K, $\lambda = 0.71073$ Å. $Z = 2$, and space group = *Pnnm* for all the compounds.
[b] $R_1 = \sum||F_o| - |F_c||/\sum|F_o|$ for $F_o^2 > 2\sigma(F_o^2)$.
[c] $wR_2 = [\sum w(F_o^2 - F_c^2)^2/\sum wF_o^4]^{1/2}$, $w^{-1} = \sigma^2(F_o^2) + (0.03F_o^2)^2$ for $F_o^2 > 0$ and $w^{-1} = \sigma^2(F_o^2)$ for $F_o^2 \le 0$.

Crystallography

Single-crystal X-ray diffraction data were collected with the use of graphite-monochromatized Mo$K\alpha$ radiation ($\lambda = 0.71073$ Å) at 153 K on a Bruker Smart-1000 CCD diffractometer (24). The crystal-to-detector distance was 5.023 cm. Crystal decay was monitored by recollecting 50 initial frames at the end of data collection. Data were collected by a scan of 0.3° in ω in groups of 606 frames each at φ settings of 0°, 120°, and 240°. The exposure time was 15 s/frame. The collection of the intensity data was carried out with the program SMART (24). Cell refinement and data reduction were carried out with the use of the program SAINT (24) and face-indexed absorption corrections were performed numerically with the use of the program XPREP (25). Then the program SADABS (24) was employed to make incident beam and decay corrections. Close examination of the individual frames revealed no evidence of supercells.

The structures were solved with the direct-methods program SHELXS and refined with the full-matrix least-squares program SHELXL (25). In these structures there are

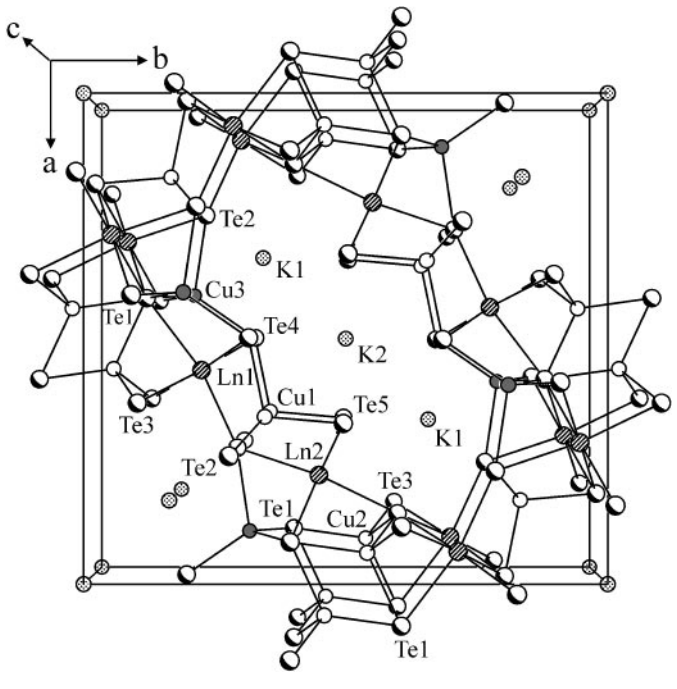

FIG. 1. View along [001] of the unit cell of $K_3Ln_4Cu_5Te_{10}$.

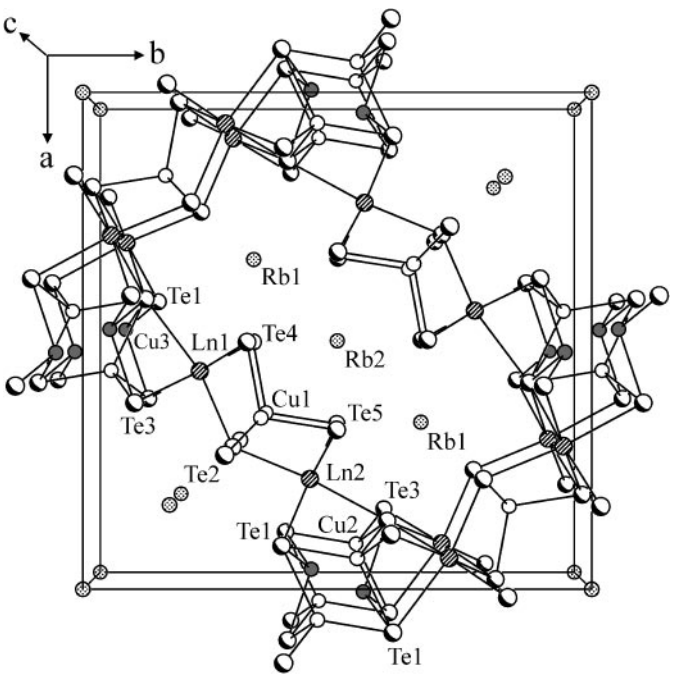

FIG. 2. View along [001] of the unit cell of $Rb_3Ln_4Cu_5Te_{10}$ (*Ln* = Nd, Gd).

TABLE 2
Atomic Coordinates[a] and Equivalent Isotropic Displacement Parameters for $K_3Ln_4Cu_5Te_{10}$ (Ln = Sm, Gd, Er)

Atom	x	y	U_{eq}[b]
$K_3Sm_4Cu_5Te_{10}$			
K1	0.8279(2)	0.1625(1)	0.0177(5)
K2	0	0	0.0256(9)
Sm1	0.06545(3)	0.28431(3)	0.0109(2)
Sm2	0.28748(3)	0.05214(3)	0.0102(2)
Cu1	0.34064(9)	0.65452(8)	0.0155(3)
Cu2	0.06452(9)	0.45995(7)	0.0162(3)
Cu3[c]	0.4061(2)	0.1898(2)	0.0164(6)
Te1	0.08409(4)	0.60481(4)	0.0096(2)
Te2	0.23132(4)	0.21389(4)	0.0110(2)
Te3	0.62926(4)	0.10199(4)	0.0103(2)
Te4	0.49699(4)	0.31759(4)	0.0128(2)
Te5	0.33184(4)	0.50603(4)	0.0113(2)
$K_3Gd_4Cu_5Te_{10}$			
K1	0.8286(2)	0.1628(2)	0.0198(6)
K2	0	0	0.025(1)
Gd1	0.06595(4)	0.28459(3)	0.0114(2)
Gd2	0.28770(4)	0.05255(4)	0.0113(2)
Cu1	0.3408(1)	0.65469(9)	0.0161(4)
Cu2	0.06429(9)	0.45975(8)	0.0163(4)
Cu3[c]	0.4066(2)	0.1898(2)	0.0169(7)
Te1	0.08458(5)	0.60527(4)	0.0102(2)
Te2	0.23107(5)	0.21435(4)	0.0123(2)
Te3	0.62996(5)	0.10219(4)	0.0113(2)
Te4	0.49735(5)	0.31678(5)	0.0128(2)
Te5	0.33037(5)	0.50561(5)	0.0122(2)
$K_3Er_4Cu_5Te_{10}$			
K1	0.8296(1)	0.16323(1)	0.0164(4)
K2	0	0	0.0244(6)
Er1	0.06652(2)	0.28540(2)	0.01013(9)
Er2	0.28819(2)	0.05309(2)	0.01003(9)
Cu1	0.34096(6)	0.65449(6)	0.0148(2)
Cu2	0.06370(6)	0.45906(5)	0.0141(2)
Cu3[c]	0.4058(1)	0.1899(1)	0.0177(4)
Te1	0.08560(3)	0.60606(3)	0.0093(1)
Te2	0.23042(3)	0.21449(3)	0.0103(1)
Te3	0.63108(3)	0.10252(3)	0.0093(1)
Te4	0.49825(3)	0.31477(3)	0.0105(1)
Te5	0.32718(3)	0.50453(3)	0.0102(1)

[a]The z coordinate of all atoms is 0.
[b]U_{eq} is defined as one third of the trace of the orthogonalized U_{ij} tensor.
[c]The occupancy of atom Cu3 is 0.50.

TABLE 3
Atomic Coordinates[a] and Equivalent Isotropic Displacement Parameters for $Rb_3Ln_4Cu_5Te_{10}$ (Ln = Nd, Gd), and $Cs_3Gd_4Cu_5Te_{10}$

Atom	x	y	U_{eq}
$Rb_3Nd_4Cu_5Te_{10}$			
Rb1	0.82925(5)	0.17050(4)	0.0161(2)
Rb2	0	0	0.0168(2)
Nd1	0.06178(2)	0.27914(2)	0.0103(1)
Nd2	0.28760(2)	0.05428(2)	0.0107(1)
Cu1	0.34512(6)	0.64932(5)	0.0159(2)
Cu2	0.06182(6)	0.46097(6)	0.0169(2)
Cu3[b]	0.4788(1)	0.0587(2)	0.0282(5)
Te1	0.08611(3)	0.60707(3)	0.0111(1)
Te2	0.22116(3)	0.21168(3)	0.0113(1)
Te3	0.62407(3)	0.10199(3)	0.0106(1)
Te4	0.50238(3)	0.32579(3)	0.0114(1)
Te5	0.32370(3)	0.50130(3)	0.0109(1)
$Rb_3Gd_4Cu_5Te_{10}$			
Rb1	0.83030(6)	0.17035(6)	0.0154(2)
Rb2	0	0	0.0169(3)
Gd1	0.06310(3)	0.28023(3)	0.0102(1)
Gd2	0.28804(3)	0.05573(3)	0.0105(1)
Cu1	0.34500(7)	0.65003(7)	0.0148(3)
Cu2	0.06165(7)	0.46066(7)	0.0152(3)
Cu3[b]	0.4764(2)	0.0530(2)	0.0254(6)
Te1	0.08740(4)	0.60934(4)	0.0107(2)
Te2	0.22157(4)	0.21289(4)	0.0110(2)
Te3	0.62480(4)	0.10149(4)	0.0100(2)
Te4	0.50245(4)	0.32248(4)	0.0108(2)
Te5	0.32097(4)	0.50121(4)	0.0106(2)
$Cs_3Gd_4Cu_5Te_{10}$			
Cs1	0.83384(6)	0.16924(5)	0.0152(2)
Cs2	0	0	0.0176(3)
Gd1	0.06741(4)	0.28383(4)	0.0122(2)
Gd2	0.29098(4)	0.05946(4)	0.0122(2)
Cu1	0.3427(1)	0.6518(1)	0.0165(4)
Cu2	0.0616(1)	0.4621(2)	0.0256(5)
Cu3[b]	0.4776(3)	0.0562(4)	0.042(1)
Te1	0.08468(6)	0.60926(6)	0.0131(2)
Te2	0.22123(6)	0.21298(6)	0.0126(2)
Te3	0.62496(6)	0.09836(6)	0.0133(2)
Te4	0.50880(6)	0.31783(5)	0.0122(2)
Te5	0.31558(6)	0.50569(5)	0.0115(2)

[a]The z coordinate of all atoms is 0.
[b]The occupancy of atom Cu3 is 0.50.

three crystallographically independent Cu sites. Refinement of the occupancies of these Cu sites led to values for atoms Cu1, Cu2, and Cu3 close to 1.0, 1.0, and 0.5, respectively. In the final refinements the occupancies of the Cu sites were fixed at these values. The resultant composition is $A_3Ln_4Cu_5Te_{10}$. Since there are no close Te···Te interactions, the oxidation states of $+1$, $+3$, $+1$, and -2 for A, Ln, Cu, and Te, respectively, may be assigned, and charge balance is achieved. Final refinements included anisotropic displacement parameters and a secondary extinction correction. Additional crystallographic details are given in Table 1. Tables 2 and 3 give positional parameters and equivalent isotropic displacement parameters, and Table 4 presents selected bond distances for $K_3Ln_4Cu_5Te_{10}$ (Ln = Sm, Gd, Er), $Rb_3Ln_4Cu_5Te_{10}$ (Ln = Nd, Gd), and $Cs_3Gd_4Cu_5Te_{10}$.

RESULTS AND DISCUSSION

The six compounds reported here crystallize in two different structure types, as illustrated for $K_3Ln_4Cu_5Te_{10}$

TABLE 4
Selected Distances (Å) for $K_3Ln_4Cu_5Te_{10}$ (Ln = Sm, Gd, Er), $Rb_3Ln_4Cu_5Te_{10}$ (Ln = Nd, Gd), and $Cs_3Gd_4Cu_5Te_{10}$

Distance	K_3Sm_4	K_3Gd_4	K_3Er_4	Rb_3Nd_4	Rb_3Gd_4	Cs_3Gd_4
*A*1–Te2 × 2[a]	3.491(2)	3.473(2)	3.446(2)	3.5672(7)	3.526(1)	3.611(1)
*A*1–Te3	3.468(3)	3.460(3)	3.437(2)	3.765(1)	3.736(1)	3.869(2)
*A*1–Te4 × 2	3.568(2)	3.552(3)	3.530(2)	3.7191(8)	3.674(1)	3.770(1)
*A*1–Te5 × 2	3.716(2)	3.693(3)	3.644(2)	3.7657(8)	3.722(1)	3.812(1)
*A*2–Te4 × 4	3.9205(7)	3.9096(9)	3.8954(8)	3.7996(4)	3.8029(7)	3.9075(8)
*A*2–Te5 × 4	3.5396(6)	3.5468(9)	3.5643(7)	3.7631(4)	3.7681(6)	3.9005(8)
*Ln*1–Te1	3.1756(9)	3.168(1)	3.1460(8)	3.2710(6)	3.2361(9)	3.271(1)
*Ln*1–Te2	3.0260(9)	3.005(1)	2.9711(8)	3.0161(6)	2.9720(9)	2.973(1)
*Ln*1–Te3 × 2	3.1600(6)	3.1393(8)	3.0991(6)	3.2333(5)	3.1887(6)	3.1888(9)
*Ln*1–Te4 × 2	3.0565(6)	3.0362(8)	2.9934(6)	3.0590(5)	3.0110(6)	3.0148(8)
*Ln*2–Te1 × 2	3.1876(7)	3.1674(8)	3.1283(6)	3.2384(5)	3.1929(6)	3.2090(9)
*Ln*2–Te2	3.0380(9)	3.024(1)	2.9879(8)	3.0327(6)	2.9909(9)	2.988(1)
*Ln*2–Te3	3.0821(9)	3.068(1)	3.0370(8)	3.1788(6)	3.1452(8)	3.167(1)
*Ln*2–Te5 × 2	3.0548(7)	3.0332(8)	2.9898(6)	3.0695(5)	3.0249(6)	3.0279(8)
Cu1–Te2 × 2	2.699(1)	2.688(1)	2.6638(8)	2.7124(7)	2.6923(9)	2.685(1)
Cu1–Te4	2.739(2)	2.726(2)	2.701(1)	2.684(1)	2.668(2)	2.656(2)
Cu1–Te5	2.659(2)	2.654(2)	2.641(1)	2.664(1)	2.649(1)	2.639(2)
Cu2–Te1	2.610(2)	2.607(2)	2.605(1)	2.637(1)	2.652(1)	2.645(2)
Cu2–Te1	2.724(2)	2.722(2)	2.710(1)	2.839(1)	2.844(2)	2.859(2)
Cu2–Te3 × 2	2.6671(9)	2.661(1)	2.6466(7)	2.6878(7)	2.6626(8)	2.675(1)
Cu3–Te1 × 2	2.659(2)	2.639(2)	2.606(1)	2.610(1)	2.627(2)	2.618(3)
Cu3–Te2 × 2	2.932(3)	2.938(4)	2.919(2)			
Cu3–Te3	2.737(3)	2.710(3)	2.668(2)	2.636(2)	2.692(3)	2.687(5)
Cu2–Cu2	2.575(3)	2.564(3)	2.542(2)	2.557(2)	2.532(2)	2.544(4)
Cu2–Cu3 × 2				2.645(1)	2.631(2)	2.654(3)
Cu2–Cu3 × 2				2.887(2)	2.789(2)	2.836(4)
Cu3–Cu3				2.219(5)	2.032(7)	2.15(1)

[a]Only *A*–Te distances less than 4.0 Å are listed.

(Ln = Sm, Gd, Er) in Fig. 1 and for $Rb_3Ln_4Cu_5Te_{10}$ (Ln = Nd, Gd) and $Cs_3Gd_4Cu_5Te_{10}$ in Fig. 2. These compounds crystallize in space group of *Pnnm* as do $Rb_3Ln_4Cu_5Se_{10}$ (Ln = Nd, Gd) (21) and $K_3Dy_4Cu_5Te_{10}$ (17). All are three-dimensional tunnel structures. The three-dimensional anionic framework is built from $LnTe_6$ octahedra and $CuTe_4$ tetrahedra. Their structures are very similar, differing in the location of the Cu3 atom. The four Cu sites in these compounds are illustrated in Fig. 3. Atoms Cu1 and Cu2 are always in Sites I and II, respectively. The Cu3 atom in $K_3Ln_4Cu_5Te_{10}$ (Ln = Sm, Gd, Er) is located in Site III, and the Cu3 and Cu4 atoms in $K_3Dy_4Cu_5Te_{10}$ are disordered over Sites III and IV. The Cu3 atom in $Rb_3Ln_4Cu_5Se_{10}$, $Rb_3Ln_4Cu_5Te_{10}$ (Ln = Nd, Gd), and $Cs_3Gd_4Cu_5Te_{10}$ is located in Site IV, but in $Rb_3Ln_4Cu_5Se_{10}$ both the Cu2 and Cu3 sites are partially occupied. The tunnel in $K_3Ln_4Cu_5Te_{10}$ (Ln = Sm, Gd, Er) (Fig. 1) contains three K^+ cations in a 16-membered ring comprising eight Cu–Te bonds and eight *Ln*–Te bonds. The tunnel in $Rb_3Ln_4Cu_5Te_{10}$ (Ln = Nd, Gd) and $Cs_3Gd_4Cu_5Te_{10}$ (Fig. 2) contains three Rb^+ or Cs^+ cations in a 20-membered ring comprising four Cu–Te bonds and 16 *Ln*–Te bonds.

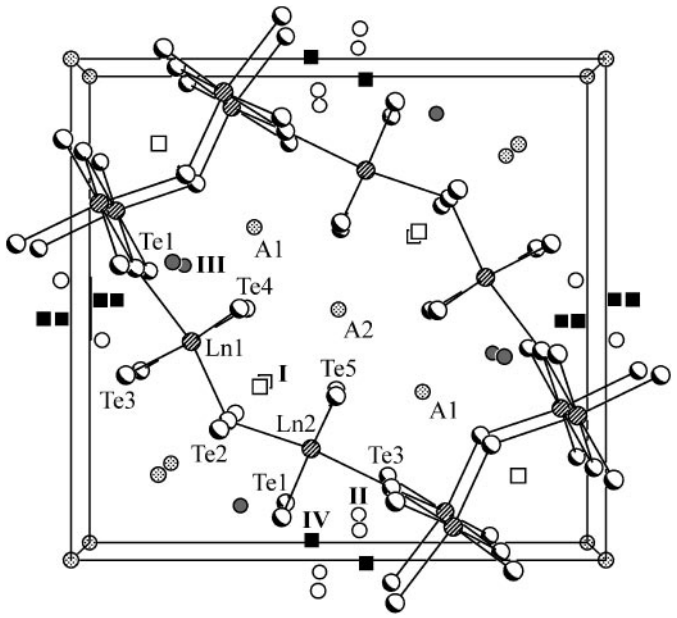

FIG. 3. Common fragment of the $A_3Ln_4Cu_5Te_{10}$ structure viewed down [001]. Here the four Cu sites (I, II, III, IV) are shown but no Cu–Te bonds are shown.

Figure 3 illustrates the common $A_3Ln_4Cu_5Te_{10}$ structure excluding Cu–Te bonds; the *Ln*/Te framework is the common motif for both structure types. The $LnTe_6$ polyhedra share edges along [001] and vertices along the other directions. The location of the Cu3 atom is related to the type of alkali-metal atoms in the tunnel. When one goes from $A = K^+$ to $A = Rb^+$ or Cs^+ the Cu3 atom moves farther out from the center of the tunnel. This is the main difference between the two structure types.

In these structures, infinite $^1_\infty[CuTe_3^{5-}]$ chains (Cu1) (Figs. 1, 2, and 4a) and infinite $^1_\infty[CuTe_2^{3-}]$ double chains (Fig. 4b) of vertex-sharing $CuTe_4$ tetrahedra run along the [001] direction. Such double chains are found in the layered compounds $NaMCuQ_3$ (M = Ti, Zr; Q = S, Se, Te) (26), $TlTiCuTe_3$ (27), and $Na_2ZrCu_2Se_4$ (28). The $Cu2Te_4$ tetrahedra in the chains in $Rb_3Ln_4Cu_5Te_{10}$ and $Cs_3Gd_4Cu_5Te_{10}$ are distorted, with Cu2–Te1, Cu2–Te1, and Cu2–Te3 (× 2) distances (Table 4) of 2.652(1) Å, 2.844(2) Å, and 2.6626(8) Å for $Rb_3Gd_4Cu_5Te_{10}$ as an example, but these tetrahedra are only slightly distorted in $K_3Ln_4Cu_5Te_{10}$, with the corresponding distances of 2.607(2) Å, 2.722(2) Å, and 2.661(1) Å for $K_3Gd_4Cu_5Te_{10}$, as an example.

Another potential tetrahedral site (two Te1, two Te3) is in the chain shown in Fig. 4c, but this site is distorted into a triangular one (two Te1, one Te3) about a Cu3 atom in the Rb and Cs structures. In $K_3Ln_4Cu_5Te_{10}$ (Ln = Sm, Gd, Er), the Cu2–Cu2 distances range from 2.542(2) to 2.575(3) Å. In $Rb_3Ln_4Cu_5Te_{10}$ (Ln = Nd, Gd) and $Cs_3Gd_4Cu_5Te_{10}$, the Cu2–Cu2 and Cu2–Cu3 distances range from 2.532(2) to 2.887(2) Å. Although the Cu3–Cu3 distances in these latter

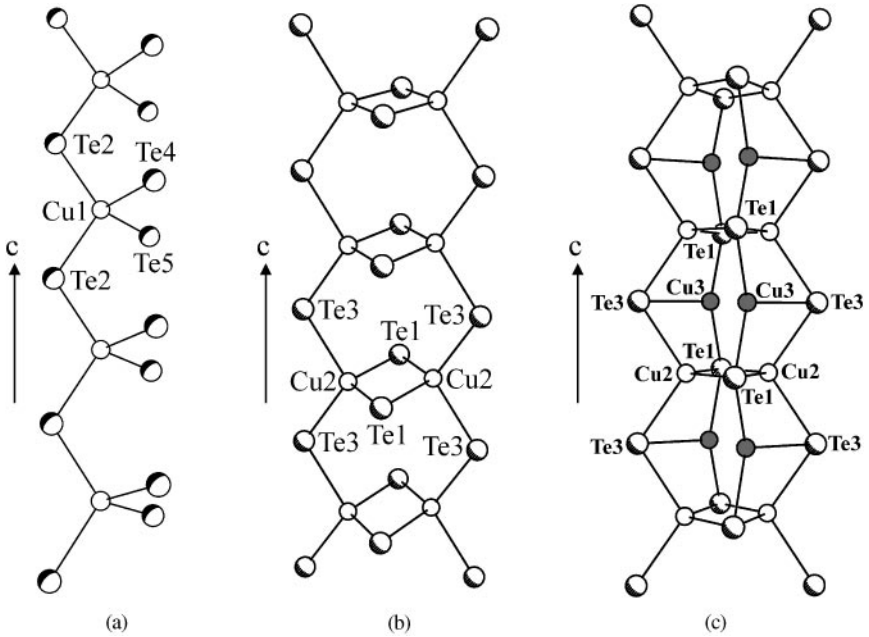

FIG. 4. (a) A $^{1}_{\infty}[CuTe_3^{5-}]$ chain of vertex-shared $CuTe_4$ tetrahedra running along [100]; (b) A $^{1}_{\infty}[CuTe_2^{3-}]$ double chain made up from two $^{1}_{\infty}[CuTe_3^{5-}]$ chains by edge-sharing along [001]; (c) A double chain with the triangularly coordinated Cu3 atoms.

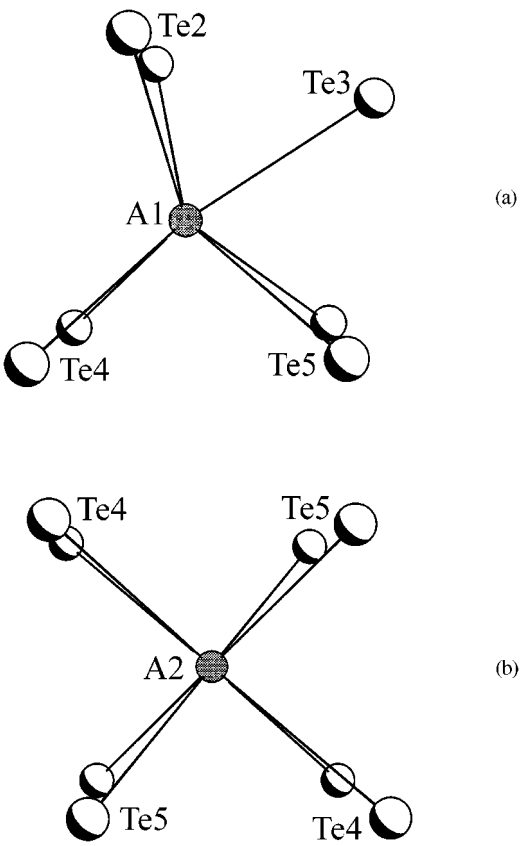

FIG. 5. (a) The $A1Te_7$ monocapped trigonal prism and (b) the $A2Te_8$ distorted cube.

structures appear to be as short as 2.032(7) to 2.219(5) Å, recall that the Cu3 sites are half occupied and such interactions need not exist. However, such short $Cu^{+}(d^{10})$–$Cu^{+}(d^{10})$ interactions have been described elsewhere (17, 21, 29–32). There are also infinite $^{1}_{\infty}[CuTe_3^{5-}]$ chains of vertex-sharing $CuTe_4$ tetrahedra (Cu3) in $K_3Ln_4Cu_5Te_{10}$ (Ln = Sm, Gd, Er). These tetrahedra are distorted with Cu3–Te1 ($\times 2$), Cu3–Te2, and Cu3–Te3 distances of 2.659(2), 2.932(3), and 2.737(3) Å, respectively, for $K_3Nd_4Cu_5Te_{10}$, as an example.

In these structures the $A1^{+}$ cations are coordinated to monocapped trigonal prisms of seven Te atoms (Fig. 5a), and the $A2^{+}$ cations are coordinated to distorted cubes of eight Te atoms (Fig. 5b). In these structures the A–Te as well as the Ln–Te distances are also normal. The latter decrease from Nd to Sm to Er, as is expected given the lanthanide contraction.

ACKNOWLEDGMENTS

This research was supported by NSF Grant DMR00-96676. This work made use of facilities supported by the MRSEC program of the National Science Foundation (DMR00-76097) at the Materials Research Center of Northwestern University.

REFERENCES

1. Y.-J. Lu and J. A. Ibers, *Comments Inorg. Chem.* **14,** 229–243 (1993).
2. E. A. Axtell III, J.-H. Liao, Z. Pikramenou, and M. G. Kanatzidis, *Chem. Eur. J.* **2,** 656–666 (1996).

3. E. A. Axtell III, J.-H. Liao, Z. Pikramenou, Y. Park, and M. G. Kanatzidis, *J. Am. Chem. Soc.* **115,** 12,191–12,192 (1993).
4. A. A. Narducci and J. A. Ibers, *J. Alloys Compd.* **306,** 170–174 (2000).
5. P. Wu and J. A. Ibers, *Z. Kristallogr.* **208,** 35–41 (1993).
6. P. Wu and J. A. Ibers, *J. Solid State Chem.* **110,** 156–161 (1994).
7. A. E. Christuk, P. Wu, and J. A. Ibers, *J. Solid State Chem.* **110,** 330–336 (1994).
8. P. Wu, A. E. Christuk, and J. A. Ibers, *J. Solid State Chem.* **110,** 337–344 (1994).
9. A. C. Sutorik, J. Albritton-Thomas, C. R. Kannewurf, and M. G. Kanatzidis, *J. Am. Chem. Soc.* **116,** 7706–7713 (1994).
10. P. Wu and J. A. Ibers, *J. Alloys Compd.* **229,** 206–215 (1995).
11. J. A. Cody and J. A. Ibers, *Inorg. Chem.* **34,** 3165–3172 (1995).
12. W. Bensch and P. Dürichen, *Chem. Ber.* **129,** 1489–1492 (1996).
13. A. C. Sutorik, J. Albritton-Thomas, T. Hogan, C. R. Kannewurf, and M. G. Kanatzidis, *Chem. Mater.* **8,** 751–761 (1996).
14. P. Stoll, P. Dürichen, C. Näther, and W. Bensch, *Z. Anorg. Allg. Chem.* **624,** 1807–1810 (1998).
15. R. Patschke, P. Brazis, C. R. Kannewurf, and M. Kanatzidis, *Inorg. Chem.* **37,** 6562–6563 (1998).
16. R. Patschke, J. Heising, and M. Kanatzidis, *Chem. Mater.* **10,** 695–697 (1998).
17. F. Q. Huang, W. Choe, S. Lee, and J. S. Chu, *Chem. Mater.* **10,** 1320–1326 (1998).
18. R. Patschke, P. Brazis, C. R. Kannewurf, and M. Kanatzidis, *J. Mater. Chem.* **8,** 2587–2589 (1998).
19. R. Patschke, P. Brazis, C. R. Kannewurf, and M. G. Kanatzidis, *J. Mater. Chem.* **9,** 2293–2296 (1999).
20. Y. Yang and J. A. Ibers, *J. Solid State Chem.* **147,** 366–371 (1999).
21. F. Q. Huang and J. A. Ibers, *J. Solid State Chem.* **151,** 317–322 (2000).
22. S. A. Sunshine, D. Kang, and J. A. Ibers, *J. Am. Chem. Soc.* **109,** 6202–6204 (1987).
23. S. A. Sunshine, D. Kang, and J. A. Ibers, *Mater. Res. Soc. Symp. Proc.* **97,** 391–396 (1987).
24. SMART Version 5.054 Data Collection and SAINT-Plus Version 6.02A Data Processing Software for the SMART System, Bruker Analytical X-Ray Instruments, Inc., Madison, WI (2000).
25. G. M. Sheldrick, "SHELXTL DOS/Windows/NT," Version 5.10, Bruker Analytical X-Ray Instruments, Inc., Madison, WI (1997).
26. M. F. Mansuetto, P. M. Keane, and J. A. Ibers, *J. Solid State Chem.* **105,** 580–587 (1993).
27. M. A. Pell and J. A. Ibers, *J. Alloys Compd.* **240,** 37–41 (1996).
28. M. F. Mansuetto and J. A. Ibers, *J. Solid State Chem.* **117,** 30–33 (1995).
29. N.-H. Dung, M.-P. Pardo, and P. Boy, *Acta Crystallogr., Sect. C: Cryst. Struct. Commun.* **39,** 668–670 (1983).
30. K. Yvon, A. Paoli, R. Flükiger, and R. Chevrel, *Acta Crystallogr., Sect. B: Struct. Crystallogr. Cryst. Chem.* **33,** 3066–3072 (1977).
31. H. Li, R. Mackay, S.-J. Hwu, Y.-K. Kuo, M. J. Skove, Y. Yokota, and T. Ohtani, *Chem. Mater.* **10,** 3172–3183 (1998).
32. S.-J. Hwu, H. Li, R. Mackay, Y.-K. Kuo, M. J. Skove, M. Mahapatro, C. K. Bucher, J. P. Halladay, and M. W. Hayes, *Chem. Mater.* **10,** 6–9 (1998).